# Estimation of local relative humidity in cathode catalyst layers of PEFC

Gazzarri, Javier; Eikerling, Michael; Wang, Qianpu; Liu, Zhong-Sheng



**Publisher's version / Version de l'éditeur:**
https://doi.org/10.1149/1.3355233
*Electrochemical and Solid-State Letters, 13, 6, pp. B58-B62, 2010-04*

*Electrochemical and Solid-State Letters,* **13** (6) B58-B62 (2010)
1099-0062/2010/13(6)/B58/5/$28.00 © The Electrochemical Society

# Estimation of Local Relative Humidity in Cathode Catalyst Layers of PEFC

**Javier Gazzarri,[a,*,z] Michael Eikerling,[a,b,*] Qianpu Wang,[a] and Zhong-Sheng Liu[a]**

[a]*National Research Council, Institute for Fuel Cell Innovation, Vancouver, British Columbia V6T 1W5, Canada*
[b]*Department of Chemistry, Simon Fraser University, Burnaby, British Columbia V5A1S6, Canada*

A simple method is presented to estimate the local relative humidity (RH) in cathode catalyst layers (CCLs) of polymer electrolyte fuel cells (PEFCs). Based on impedance measurements under different experimental conditions, this technique provides a means to estimate the average value for RH using a correlation with the catalyst layer effective proton resistance. At zero current, a fully humidified anode raises the RH inside the CCL from a nominal 30% to almost 70%. A current density of up to 0.4 $A/cm^2$ also humidifies the cathode, while drying is observed between 0.4 and 1.0 $A/cm^2$.
 [DOI: 10.1149/1.3355233] 

Manuscript submitted November 10, 2009; revised manuscript received December 23, 2009. Published April 2, 2010. This was Paper 1017 presented at the Vienna, Austria, Meeting of the Society, October 4–9, 2009.

High proton conductivity in cathode catalyst layers (CCLs) of polymer electrolyte fuel cells (PEFCs) is desirable to ensure a large reaction penetration depth, which in turn enhances catalyst utilization and overall performance. Sufficiently high proton conductivity relies on an appropriate humidification of the ionomer in the catalyst layer. Several cell phenomena concomitantly take place within the CCL domain, making the local water activity and, thus, proton conductivity very difficult to determine accurately. Such phenomena include ionomer humidification from the cathode feed stream, electrochemical water production, electro-osmotic drag, vapor diffusion, hydraulic flux of liquid water, and evaporation and condensation processes.

A thorough understanding of water transport in the CCL and its influence on performance lie at the heart of improving the design of the membrane electrode assembly (MEA) that can meet current demands for decreasing cost and improving power density and voltage efficiency. Moreover, understanding the conditions for an optimal water balance in the CCL could simplify the overall layout of the fuel cell system. A rather desirable simplification would be the elimination of external gas humidifiers, which would significantly reduce the balance of plant, while demanding sufficient self-humidification of the proton-conducting and porous domains of the MEA.

Under the steady-state operation with fluxes of liquid water and water vapor, as well as water production, relative humidity (RH) should be considered a spatially strongly varying function in the MEA. Equating local RH in the CCL to the humidity in the inlet gas stream is inadequate in the case of different humidification on each side of the membrane, or in the presence of a finite current density. Because direct measurements of the local humidity in the CCLs are not feasible, there is a dire need for a technique that relates the actual RH to a measurable local physical property.

In this article, we present a method to estimate the average RH inside the CCL based on impedance spectroscopy measurements. It exploits the correlation between the proton resistance, water content in the CCL, and water vapor activity. In our approach, we neglect the contribution from the anode to polarization losses. For the sake of simplicity, we assume that there is no temperature gradient across the cell.

This article is organized as follows. First, the impedance data in a hydrogen/nitrogen atmosphere and equally humidified electrodes are analyzed to obtain an estimate of the effective proton resistance of the CCL. This correlation gives a baseline for the relation between effective proton resistance and RH. Second, the measurement is repeated for a dry (30% RH) cathode and an increasingly humid anode using the same gas feed composition. The measured proton resistance is then used to calculate the average actual humidity based on the previously measured baseline. The method is then applied to PEFC operation at a finite current density under oxygen atmosphere, where capabilities and limitations of the method's applicability become apparent.

## Experimental

The impedance spectra of a PEFC assembly (Nafion 211 membrane, Pt loading of 0.4 $mg/cm^2$, mass ratio of ionomer to carbon (I/C ratio) of 0.79, mass ratio of Pt to Ketjen black carbon of 0.46 were measured under several humidity and current density conditions, in nitrogen or oxygen (cathode side) and hydrogen (anode side). The nominal cell temperature was 80°C in all cases, and the flow rates to the anode and cathode were 0.5 and 1.0 L/min, respectively. The cell active area was 5 $cm^2$. Table I summarizes the humidity conditions for all cases.

During the hydrogen/nitrogen experiment, the dc potential was held at 0.45 V to avoid unwanted side reactions such as hydrogen and $OH^-$ adsorption–desorption. Before each impedance measurement, the cell conditions were held unchanged for approximately 30 min to ensure a steady state measurement. The total gas pressure on both sides of the cell was 101.3 kPa (atmospheric) at all times.

The method presented here consists of estimating an average humidity within the CCL by measuring its total proton resistance and inferring the actual humidity using a previously determined humidity vs resistance relation. This baseline was first obtained by measuring the proton resistance of the CCL under equal humidification conditions at both the anode and the cathode, in which case it can be assumed that the actual CCL humidity coincides with the externally set RH. Subsequent measurements of resistance under unequal humidity conditions were then used to determine the actual humidity from the baseline data set.

An underlying assumption of this method is that the vaporization–condensation rate is fast compared to other water transport phenomena, allowing us to relate proton resistance directly to RH. In principle, resistivity is a direct function of water content and not of RH. For rapid vaporization–condensation, the relation between RH and water content is given by the sorption isotherm, which can be employed to eliminate water content. Another underlying assumption is that the proton resistivity in the catalyst layer can be well represented by an effective value. This implies that the variations in the liquid water saturation and, consequently, in the ionomer hydration are moderate. Obviously, the method would work best for constant liquid saturation and rapid vaporization exchange. It would still give a meaningful estimate of the RH in the catalyst layer if the gradient in the liquid water saturation were small in the parts of the layer that make the main contribution to the proton resistance. Current work in our group focuses on water transport

* Electrochemical Society Active Member.
z E-mail: Javier.Gazzarri@nrc-cnrc.gc.ca

**Table I. Anode and cathode stream humidity for the seven tested cases. $T$ = 80°C. Flow rates: anode, 0.5 L/min and cathode, 1 L/min.**

| | | | | | | | |
|---|---|---|---|---|---|---|---|
| Anode relative humidity | 100 | 70 | 50 | 30 | 100 | 70 | 50 |
| Cathode relative humidity | 100 | 70 | 50 | 30 | 30 | 30 | 30 |

phenomena in the CCL, including liquid permeation, vapor diffusion, and vaporization exchange under diverse experimental conditions. The results of these efforts would provide detailed distributions of liquid water saturation and water vapor in the CCL; they would allow testing the above-mentioned assumptions of quasi equilibrium between liquid and vapor in the CCL. Moreover, the measured impedance was assumed to originate solely at the cathode, with a negligible anode contribution.

## Results and Discussion

*Cathode humidification at zero current.*— The first step toward estimating the local RH using this method is to characterize the CCL in terms of its effective proton resistance. In this work, the term effective proton resistance denotes the proton resistance averaged over the CCL thickness, which depends on the distribution and self-organized structure of the ionomer in the CCL and the degree of liquid saturation. The proton resistance can be found from the impedance response of the CCL.[1-3]

Figure 1 shows the result of the impedance measurement in a $H_2$ (anode)–$N_2$ (cathode) atmosphere for the 30% setup RH on both sides of the cell and illustrates the procedure for the estimation of the effective proton resistance of the CCL. When the polarization resistance is much larger than the proton resistance (as is the case for a $H_2$–$N_2$ experiment), the CCL impedance $Z$ can be approximated by[1]

$$Z \approx \sqrt{\frac{R^{H^+}}{j\omega C_{dl}}}\coth\left(\sqrt{j\omega C_{dl}R^{H^+}}\right)$$

Here, $R^{H^+}$ is the average proton resistance ($\Omega$ cm$^2$), $C_{dl}$ is the double-layer capacitance (F/cm$^2$), and $\omega$ is the angular frequency (1/s). Two distinct regions characterize an impedance spectrum with this functional form a straight line at high frequency, theoretically at 45° with respect to the real axis and representative of proton transport, and a vertical line at low frequency, typical of capacitive behavior. Double-layer charging dominates the high frequency portion, and the impedance dependence on frequency reflects the increasing ac signal penetration depth. Within the low frequency region, the ac signal penetrates the whole catalyst layer thickness; thus, its real part is proportional to the total proton resistance contribution, while its imaginary part reflects almost purely capacitive charge and discharge behavior. The real axis intercept of the typical impedance spectrum shown in Fig. 1 corresponds to the sum of the membrane and electronic resistance contributions and the contact resistances between the MEA layers. The extrapolation of the asymptotic behaviors in the low and high frequency regions (straight lines in Fig. 1) results in an intercept at intermediate frequencies. The projection of the intercept onto the real axis minus the high frequency intercept (Fig. 1), multiplied by 3, constitutes the total proton resistance of the CCL.[1,2]

Figure 2 shows the set of resistance data for equal humidifications, namely, 100–100, 70–70, 50–50, and 30–30. Applying the aforementioned procedure to these cases results in four values of CCL effective proton resistance and four values of membrane + other ohmic resistances. These four cases constitute the calibration baseline.

Although, in theory, the low frequency impedance in this experiment should be purely capacitive (a vertical line in the Nyquist diagram), a deviation from this ideal state is expected due to the traces of oxygen in the cathode stream, giving rise to a finite dc resistance in the low frequency limit and therefore a deviation from a vertical line within the range of frequencies of interest. Deviations from a 45° angle in the high frequency limit have been attributed to

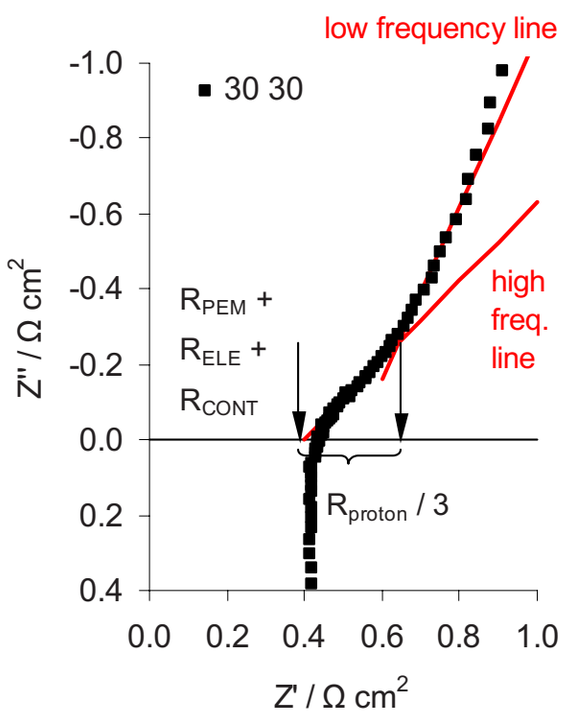


**Figure 1.** (Color online) Impedance spectrum in $H_2/N_2$ atmosphere for the 30% inlet RH on both anode and cathode sides, illustrating the method for extracting the proton resistance. The straight lines extrapolating low and high frequency behaviors are determined by visual inspection. The intersection of the line in the high frequency limit with the real axis determines the membrane resistance plus electronic and contact resistance contributions, and the real component at the intersection of both lines, minus the high frequency limit, is proportional to the total proton resistance contribution of the CCL.

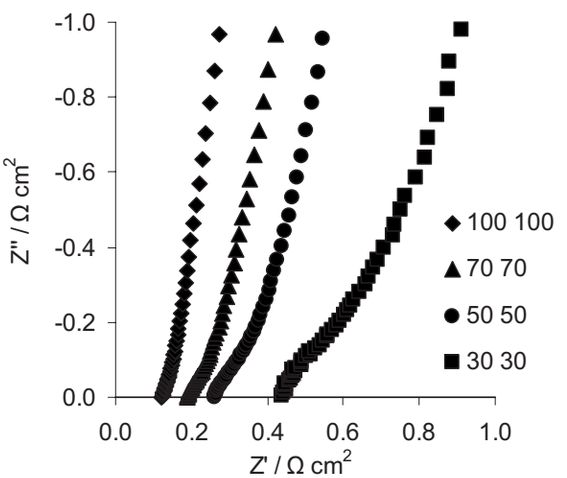


**Figure 2.** Impedance in $H_2/N_2$ atmosphere (zero dc current) under conditions of equal relative humidity on anode and cathode used for the determination of the baseline relation between proton resistance and RH (Table I, columns 1–4). Labels indicate RH (in percent) at anode and cathode.

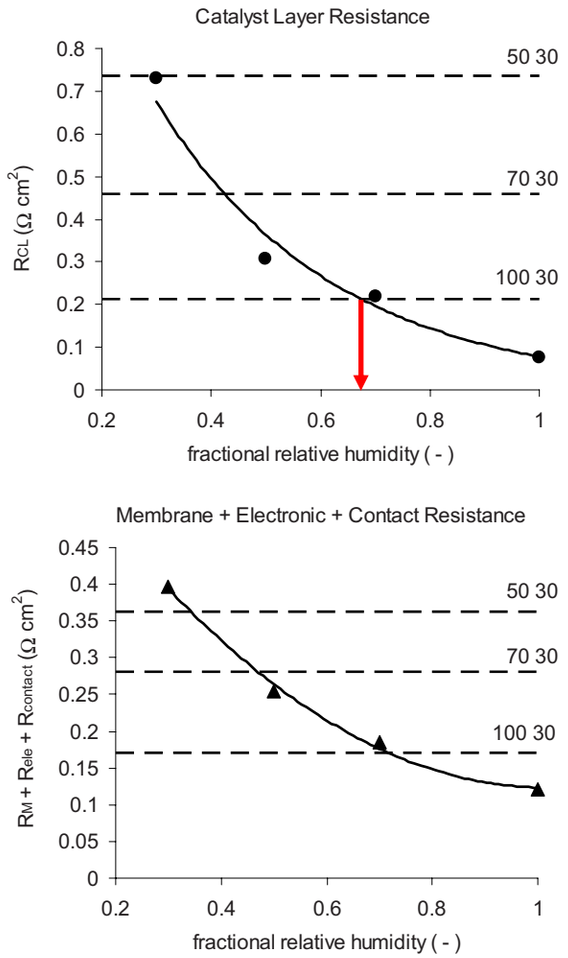


**Figure 3.** (Color online) (a) Average proton resistance of the CCL and (b) membrane resistance plus electronic and contact resistances as a function of RH (equilibrated conditions). The solid lines constitute the baseline used to estimate apparent local RH for a given value of proton resistance. Horizontal dashed lines indicate experimentally determined resistances of PEM and CCL, respectively, for cases with different RHs on both sides ($RH_{anode}$ and $RH_{cathode}$, specified in the labels); projection of intercepts between horizontal lines and relevant baseline onto the abscissa provide effective equilibrium RHs for (a) PEM and (b) CCL. The arrow in (a) points at the local average humidity corresponding to 100/30.

nonuniformities in the proton resistance[4-6] and hierarchical branching of pores (Ref. 7, p. 78), although it is not clear whether these causes apply to the present case.

The CCL proton resistance and the bulk resistance of the polymer electrolyte membrane (PEM) strongly depend on both the cathode and anode inlet RHs, as shown in Fig. 3a and b. Figure 3a shows the effective catalyst layer proton resistance as a function of RH for the four baseline cases (●), and the three horizontal dashed lines indicate the resistance determined for the unequal humidification, as indicated in the plot. Our calculation of the proton resistance agrees well with the results reported in Fig. 8 of Ref. 8 if the resistivity reported in that work (from 600 Ω cm at 35% RH to 100 Ω cm at 75% RH for an IC ratio of 0.79) is affected by an average nominal thickness of 12 μm, resulting in CCL proton resistances from 0.72 Ω $cm^2$ at 35% RH to 0.12 Ω $cm^2$ at 75% RH. Similarly, Fig. 3b shows the resistance of the bulk membrane plus other ohmic resistance contributions (electronic + contact) for the baseline cases (▲) and the calculated resistances for 100–30, 70–30, and 50–30 RH as horizontal dashed lines.

**Table II. Predicted RH inside the CCL and effective RH in equilibrium with the membrane for a nominal 30% cathode RH. These three cases correspond to the cases in Table I with unequal humidity conditions.**

| | Anode stream RH | | |
|---|---|---|---|
| | 50 | 70 | 100 |
| Local RH in the CCL | 27 | 43 | 68 |
| RH in equilibrium with the membrane | 34 | 47 | 71 |

The CCL proton resistance decreases with increasing inlet RH on both sides as expected. More remarkably, proton resistance at the cathode also decreases with increasing anode inlet RH when a constant 30% humidity is set at the cathode. The latter observation is an indication of a very effective water transport process through the membrane and the cathode. The bulk membrane resistance shows a similar trend.

*Estimation of local RH at the CCL at zero current.*— The second step of this method is to estimate the average CCL humidity. The baseline determined by the four equal-humidity cases used to generate Fig. 3a and b relates the CCL effective proton resistance (Ω $cm^2$) and fractional relative humidity $x_{RH}$ (nondimensional) by an empirical relation

$$R_{CL} = 1.70\ \exp(-3.08x_{RH})$$

These quantities correlate with $r^2 = 0.98$ using four data points. Using the high frequency intercepts, a separate empirical relation is obtained for the membrane + electronic + contact resistance (Ω $cm^2$)

$$R_{MEM} + R_{ele} + R_{cont} = 0.525x_{RH}^2 - 1.068x_{RH} + 0.667$$

The correlation factor is $r^2 = 0.99$ for the four data points. The solid lines in Fig. 3a and b correspond to the fitting functions and constitute the baseline of our calculation. The unequal anode and cathode RHs correspond to the nonuniform water distributions across the MEA. We assume that, nevertheless, water distributions inside of the PEM and CCL can be presented reasonably well by single effective values. This implies that variations in liquid water saturation inside of each of these media are negligible. The effective liquid water saturation of PEM or CCL corresponds to an effective RH of water vapor that would be in equilibrium with the PEM at the given water content. This effective equilibrium RH deviates from the real prevailing RH due to vaporization/condensation fluxes at liquid/vapor interfaces. The effective equilibrium RH value can be determined from the plots in Fig. 3; it is given by the intercept between the dashed line, representing the unequal anode/cathode RH conditions, and the baseline, projected onto the real axis. This step is indicated in Fig. 3a, where the arrow indicates the RH calculated at the 100% $RH_{anode}$/30% $RH_{cathode}$ conditions. Thereafter, the equilibrium sorption isotherms of the PEM and CCL could be used to relate the effective equilibrium RH values, thus determined, to liquid water saturations.

Table II shows the predicted local effective equilibrium RHs for the three nonequal humidifications, both for the CCL (first row) and the membrane (second row). The effective equilibrium RH for a bulk polymer (second row) represents the RH of water vapor that is in equilibrium with the membrane to yield the observed proton resistance. It can be related to the real water content in the membrane using the sorption isotherm.

The method suggests the suitability of impedance spectroscopy for the indirect estimation of RH and liquid saturation in components such as the CCL, inaccessible to a humidity probe. Higher humidification at the anode side incurs a water flux toward the cathode, which leads to a rise in the water content at the cathode side of the PEM and an increase in the liquid saturation of the CCL, improving the proton conductivity of the latter. The low effective equi-

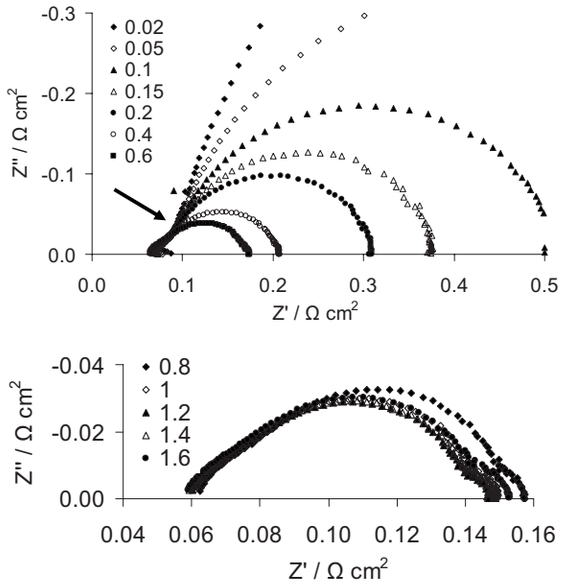


**Figure 4.** Impedance spectra at different current densities (legend, in A/cm$^2$) for the case of $H_2$ (anode)/$O_2$ (cathode), both at 100% RH. (a) 0.02–0.6 A/cm$^2$. Although the overall impedance spectrum shape shows strong dependence on current density, the high frequency linear region remains largely unchanged. The arrow shows the transition from the double-layer charging regime to the ORR regime. (b) 0.8–1.6 A/cm$^2$.

librium RH of 27% in the first row of Table II, which lies below the nominal cathode RH equal to 30%, is due to the error associated with this method (±5%). This estimation for the method's uncertainty was done choosing two extreme cases of pair of points defining the low frequency asymptotic line shown in Fig. 1. Results confirm that the effective equilibrium RH and thus the real liquid saturation in the CCL depend strongly on the anode RH and the water transport properties of the PEM. A fully humidified anode and a highly water-permeable membrane can keep the cathode in a well-humidified state, even at low nominal RH on the cathode side. This is especially so for thin (~10 μm) membrane electrolytes, which minimize the membrane bulk resistance to water crossover. The similarity between the effective equilibrium RH values for the PEM and CCL (row 1 vs row 2 in Table II) indicates a facile liquid water transport in the ionomer and the pores of the catalyst layer. Moreover, this finding suggests that the resistance to liquid water transport at the PEM/CCL interface is negligible.

*Catalyst layer RH estimation at nonzero current density.*— A case of interest for the application of this method is that of finite current density because water is produced and transported across the layers of the MEA as a consequence of this current. We repeated the impedance measurement in $H_2/O_2$ at current densities ranging between 0.02 and 1.6 A/cm$^2$. The procedure herein described is directly applicable to $H_2$/air. When current density is not close to zero, the impedance spectrum has a semicircular or half teardrop shape as a result of the interplay between charge and mass transport resistances of the composite media and the faradaic resistance of the oxygen reduction reaction (ORR). Increasing the cell current density decreases the proton resistance by humidification of the ionomer and also results in a reduction of the ORR faradaic resistance. As a consequence, the reaction penetration depth, or catalyst layer utilization, decreases with increasing current density. This results not only in a decrease in the size of the impedance arc, but also in the gradual disappearance of the transition point between the 45° straight line regime at high frequency ($C_{dl}$ charging regime) and the semicircular regime at medium to low frequency (ORR dominated regime). Figure 4 exemplifies this statement showing the impedance

**Table III. Total double-layer capacitance (F/cm$^2$) as a function of inlet RH (the same at both electrodes) for $H_2/N_2$, determined via $R^{H^+}$ using the method shown in Fig. 1.**

| | RH (%) | | | |
|---|---|---|---|---|
| | 30 | 50 | 70 | 100 |
| $C_{dl}$ | 0.0225 | 0.0223 | 0.0284 | 0.0288 |

measured in $H_2/O_2$ and fully humidified inlet gases. The arrow in Fig. 4a indicates the approximate transition frequency at which the impedance changes from the $C_{dl}$ regime to the ORR regime. The legend indicates the current density in A/cm$^2$. In this case, the transition current density is approximately 0.4 A/cm$^2$. Above this current density, there is no observable slope change in the Nyquist plot of the impedance between the two regimes described above, reflecting a signal penetration depth smaller than the catalyst layer thickness.

If this transition is not apparent (e.g., Fig. 4b), the proton resistance needs to be estimated in some other way. As reported by Eikerling and Kornyshev in Ref. 1, the impedance at high frequency depends on proton resistance and double-layer capacitance with this functional form

$$\underset{\omega\to\infty}{Z} \approx \sqrt{\frac{R^{H^+}}{j\omega C_{dl}}}$$

This relation means that proton resistance may be calculated if $C_{dl}$ is known by other means. If we assume that $C_{dl}$ remains constant with current density, we can easily estimate $R^{H^+}$ using, for example, the imaginary part of the equation above (only valid at high frequency) and the $C_{dl}$ calculated at the RH values used to construct the calibration baseline using the $H_2/N_2$ data

$$\mathrm{Im}\left(\underset{\omega\to\infty}{Z}\right) \approx \sqrt{\frac{R^{H^+}}{2\omega C_{dl}}} \Rightarrow R^{H^+} = 2\omega C_{dl}\left[\mathrm{Im}\left(\underset{\omega\to\infty}{Z}\right)\right]^2$$

Table III shows the four capacitance values calculated in this way. Once the average $C_{dl}$ is known at each humidity condition, we can estimate the proton resistance using the equation shown above.

Figure 5 shows the average proton resistance of the catalyst layer

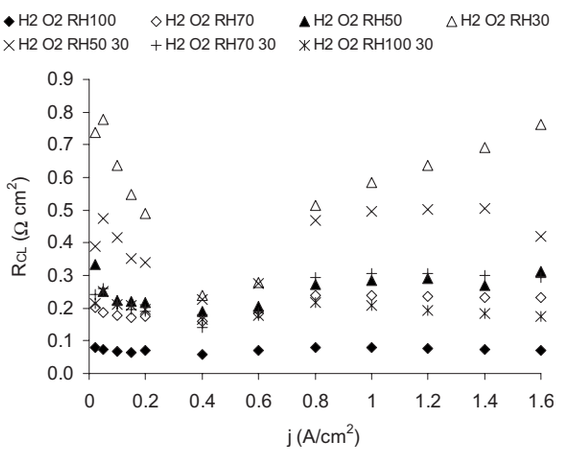


**Figure 5.** Catalyst layer resistance measured in $H_2/O_2$ atmosphere as a function of current density. Legend indicates the RH of the feed gas stream. RH *X* means *X*% RH on both sides. RH *X Y* means *X*% $RH_{anode}$ *Y*% $RH_{cathode}$. Especially at low cathode RH conditions, the measured RH decreases up to 0.4 A/cm$^2$ likely because of water production at the cathode and then increases and levels off.

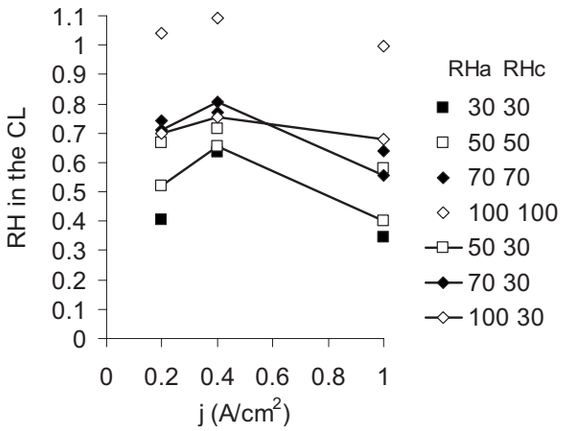


**Figure 6.** Calculated RH at the CCL for different gas stream humidifications (legend) at 0.2, 0.4, and 1.0 A/cm$^2$. $H_2$ (anode)/$O_2$ (cathode) atmosphere. Although RH shows an initial increase, it decreases from 0.4 to 1.0 A/cm$^2$ likely due to thermal effects on humidity.

as a function of current density for differently humidified gas streams (legend) estimated using this method. The average CCL proton resistance decreases between 0 and 0.4 A/cm$^2$ and then increases again to different degrees depending on the humidification conditions. The decrease is most likely the result of self-humidification due to electrochemical water production. We attribute the subsequent increase to an increase in temperature, as explained in the next paragraph.

Using the baseline described in the previous section, along with these proton resistance values, we calculated the effective equilibrium RH in the CCL, now as a function of both gas stream humidity (legend) and current density. Figure 6 shows how the effective equilibrium RH varies with the current density for all tested gas feed humidity conditions. At current densities in the range of 0–0.4 A/cm$^2$, the calculated effective equilibrium RH increases due to water production. The effective equilibrium RH decreases beyond 0.4 A/cm$^2$ for all the cases considered here. The corresponding decrease in the liquid saturation at higher current densities can be attributed to a balance between humidification due to water generation and drying due to temperature increase. At 80°C ($p_{sat}$ = 47.3 kPa), it takes a temperature rise of ~10°C to increase $p_{sat}$ by 50%, roughly the increase needed to decrease RH from 60 to 40%. These results are important for the performance of the experiments because they indicate that there are several ways in which the catalyst layer humidity may deviate from the set point humidity.

## Conclusions

A method is presented to estimate the local effective equilibrium RH and thus the liquid water saturation inside a CCL using impedance spectroscopy. It is applicable for the practically important case of different nominal RHs on the anode and cathode sides of the MEA. Results indicate that within the method's uncertainty, the effective equilibrium RH and thus the saturation level on the cathode side are significantly higher than the values corresponding to the nominal (externally provided) RH at the cathode. Due to the highly efficient liquid water transport in the PEM and CCL, the RH in the CCL is strongly dependent on the anode RH. At zero current density, nominal RHs of 100% at the anode and 30% at the cathode yielded an effective equilibrium RH of 68% in the CCL and at the CCL/PEM interface. In the presence of a finite current density, the calculated CCL humidity increases over the range of 0 and 0.4 A/cm$^2$ due to water production and then decreases presumably due to the competing effects of water production and temperature rise. It is important to consider these effects when performing experiments controlling humidity by setting the gas feed humidity, because the real liquid water saturation may differ significantly from the value that corresponds to the set RH.

## Acknowledgments

J.G. is grateful to Makoto Adachi and Dr. Jennifer Peron for fruitful discussions.

*National Research Council of Canada assisted in meeting the publication costs of this article.*

## References

1. M. Eikerling and A. A. Kornyshev, *J. Electroanal. Chem.*, **475**, 107 (1999).
2. R. Makharia, M. Mathias, and D. Baker, *J. Electrochem. Soc.*, **152**, A970 (2005).
3. M. Eikerling, A. A. Kornyshev, and A. A. Kulikovsky, in *Encyclopedia of Electrochemistry 5*, Chap. 8.2, D. D. Macdonald and P. Schmuki, Editors, pp. 447–543, VCH-Wiley, Weinheim (2007).
4. M. Lefebvre, R. Martin, and P. Pickup, *Electrochem. Solid-State Lett.*, **2**, 259 (1999).
5. G. Li and P. Pickup, *J. Electrochem. Soc.*, **150**, C745 (2003).
6. X. Ren and P. Pickup, *Electrochim. Acta*, **46**, 4177 (2001).
7. J. R. MacDonald and E. Barsoukov, *Impedance Spectroscopy*, 2nd ed., p. 58, John Wiley & Sons, New York (2005).
8. Y. Liu, M. Murphy, D. Baker, W. Gu, C. Ji, J. Jorne, and H. Gasteiger, *J. Electrochem. Soc.*, **156**, B970 (2009).